Iranian Journal of Chemistry and Chemical Engineering (IJCCE)

Optimizing Leaching Parameters for Copper Extraction from Chalcopyrite using [Bmim][HSO_4] Ionic Liquid

Moazzami, Yaser[1]; Shafaei Tonkaboni, Sied Ziaedin[2]; Gharabaghi, Mehdi[3,*+]

[1]Ph.D Student, School of Mining Engineering, College of Engineering, University of Tehran, Tehran, I.R. IRAN.

yaser.moazzami@ ut.ac.ir

[2]Professor, School of Mining Engineering, College of Engineering, University of Tehran, Tehran, I.R. IRAN.

zshafaie@ut.ac.ir

[3]Associate Professor, School of Mining Engineering, College of Engineering, University of Tehran, Tehran, I.R. IRAN.*

gharabaghi@ut.ac.ir

ABSTRACT: *Today, there has been a significant emphasis on developing sustainable and environmentally friendly processes in various industries, including hydrometallurgy. This study focuses on the process of leaching chalcopyrite concentrate using an ionic liquid called 1-butyl-3-methyl-imidazolium hydrogen sulfate ([Bmim][HSO_4]). To study the impact of various parameters on the chalcopyrite leaching, such as temperature, [Bmim][HSO_4] and H_2O_2 concentration, speed of stirring, solid-to-liquid ratio, and their interactions, design expert software was used. Employing the CCD layout of RSM matrix, 32 experiments were designed and executed. The results showed that the temperature, oxidizing agent concentration, and ionic liquid concentration, as well as the interaction between the oxidizing agent concentration with the ionic liquid concentration and temperature, have the most significant effect on the dissolution of chalcopyrite. Also, the highest amount of copper extraction (90.32%) was obtained at 40°C using 40% [Bmim][HSO_4], 30% H_2O_2, ratio of solid-to-liquid 10 g/l, and speed of stirring 300 rpm. The examination of kinetic studies employing the SCM showed that the process of extracting copper from chalcopyrite utilizing $BmimHSO_4$ ionic liquid follows from the chemical reaction, and in this condition, the activation energy is 49.61 kJ/mol. Finally, evaluation of surface morphology and characteristics of leaching residue using XRD and SEM/EDX analyses revealed that most of the $CuFeS_2$ has been dissolved and elemental sulfur is the major solid product that exists in the chalcopyrite leaching residue.*

KEYWORDS: *Chalcopyrite, Leaching, Ionic Liquids, Design Of Experiment (DOE), Optimization.*

* To whom correspondence should be addressed.

+ E-mail: gharabaghi@ut.ac.ir, m.gharabaghi@gmail.com

INTRODUCTION

Chalcopyrite, with the chemical formula of $CuFeS_2$, exhibits notable resistance to leaching due to alterations in its surface properties, chemical structure, and the development of a passive porous layer on its surface. [1, 2]. Hence, extensive research has been done on the leaching of this mineral, and due to its low solubility, different solvent-based leaching processes have been developed such as, chloride leaching [3], ammonia leaching [4], bioleaching [5], and pressure sulfate leaching [6] for the extraction of copper from chalcopyrite. Nevertheless, due to their low yields, the necessity for high temperatures and pressures, challenges in separating solvents from products and lack of achieving complete recovery, environmental risks, and the noteworthy costs linked to the management of these solvents, there are some controversies about the applicability [7-9]. As a result, there is a growing need for novel processes to drive sustainable and environmentally friendly advancement within the copper hydrometallurgical industry. These processes aim to produce copper under ambient atmospheric conditions, utilizing low temperatures, minimal energy, and low acid consumption, all while avoiding pollutant emissions. In light of this objective, using ionic liquids for copper extraction from chalcopyrite has garnered attention, prompting a series of research studies in this domain [9, 10].

Ionic liquids represent a distinctive category of salts that have sparked a revolution in both research centers and chemical industries in recent years. This novel class of chemical compounds exhibits unique properties, dissolving both organic and inorganic compounds while remaining practically non-volatile, non-flammable, and thermally stable. These characteristics make them promising green alternatives to traditional organic and inorganic solvents in various chemical processes. [8, 11-13]. In ionic liquids, unlike molecular solvents, each particle possesses a singular ionic charge. As implied by their name, they comprise entirely ionic compounds composed of diverse cations and anions. Typically, cations are represented by bulky organic compounds bearing a positive charge, while anions are inorganic and considerably smaller in size compared to cations, carrying a negative charge. The size disparity between anions and cations leads to a weak bond between the two components of ionic liquids. Consequently, these compounds exhibit a low melting point [13-16]. The most common cations used in ionic liquids are imidazolium, pyridinium, ammonium, phosphonium, and sulfonium. The variety of anions is greater than that of cations. Some of the anions used in ionic liquids include hexafluorophosphate, tetrafluoroborate, bis(trifluoromethylsulfonyl)imide, trifluoromethane sulfate, methyl sulfate, dicyanamide, halogens, acetates, and dimethyl phosphate [17].

Today, ionic liquids have gained extensive use in various fields due to their desirable characteristics, such as minimal environmental pollution, complete recyclability, and low melting temperatures. These attributes have created a non-aqueous liquid organic environment, enabling the execution of numerous organic reactions. However, they are mainly used as green solvents instead of volatile solvents [18]. Research conducted on the leaching of gold and silver [19-21], rare earth elements [22, 23], and metal oxides [13, 24-26]using ionic liquids as solvents has demonstrated the significant capability of these liquids in dissolving metals and metal oxides [10].

McCluskey employed 1-butyl-3-methylimidazolium tetrafluoroborate ($[BMIM]BF_4$) as an ionic liquid and iron tetrafluoroborate ($Fe(BF_4)_3$) as an oxidizing agent for the oxidation of organic substrates. [27]. They showed that 90% copper extraction can be reached within 8 h at 100°C. In another study conducted in 2007, the extraction of copper from primary chalcopyrite containing about 20% Cu and 34% Fe was investigated using $[Bmim][HSO_4]$ ionic liquid by Whitehead et al. [8]. Based on this study, these researchers stated that increasing the concentration

of ionic liquid from 10% by weight in water to 100% at 70°C increases the extraction of copper from 55% to 87%, and under these conditions, the maximum extraction of iron is 8%. These researchers attributed the heightened copper extraction with rising concentration of ionic liquid to heightened acidity, greater ionic strength, and increased oxygen solubility within the ionic liquids. They also proposed that due to the high solubility of oxygen and its combination with sulfide ions, the possibility of forming soluble sulfate species instead of elemental sulfur is increased, hence the leaching process is not limited by the formation of elemental sulfur surface coating [8]. In 2009, Dong et al. investigated the leaching of chalcopyrite concentrate [28]. These researchers reported that by increasing the concentration of ionic liquid from 10% to 100%, the copper extraction at 70 °C increased from 52% to 88% following the 24-hour reaction. This aligns with Whitehead's observations, suggesting consumption of hydrogen and oxygen during the process. [8]. They mentioned that the rise in copper extraction, resulting from increasing the concentration of the ionic liquid from 10% to 60%, can be attributed to more dissolved oxygen and higher acidity. Conversely, the slight increase in copper extraction when increasing the concentration of the ionic liquid to 100% is likely due to the rise in viscosity and the limitations in the diffusion of the ionic liquid. Further analysis of the leaching residue by XRD and SEM methods showed that chalcopyrite was dissolved, its copper and iron elements were released, and the elemental sulfur was formed around the chalcopyrite core. They also observed that Fe^{2+} and Fe^{3+} were present in the leaching liquor, and the ratio of concentration of ferric to ferrous was between 0.4 and 1.1. Therefore, they proposed reaction (1) as the primary reaction of chalcopyrite dissolution in [Bmim][HSO_4], which is obtained from the sum of reactions (2) and (3).

$$CuFeS_2 + 4Fe^{3+} \rightarrow Cu^{2+} + 5Fe^{2+} + 2S \quad (1)$$

$$4Fe^{2+} + 4H^+ + O_2 \rightarrow 4Fe^{3+} + 2H_2O \quad (2)$$

$$CuFeS_2 + 4H^+ + O_2 \rightarrow Cu^{2+} + Fe^{2+} + 2S^0 + 2H_2O \quad (3)$$

They also measured the activation energy and showed that the activation energy of chalcopyrite dissolution in the presence of ionic liquid is 69.4 kJ/mol. As a result, they concluded that the dissolution reaction of chalcopyrite in ionic liquids controls with surface electrochemical processes. Carlesi et al. [10] investigated the leaching of chalcopyrite from sulfide mineral using sulfuric acid, 1-hexyl-3-methyl-imidazolium hydrogen sulfate (IL_1), and 1-butyl-3-methyl-imidazolium hydrogen sulfate (IL_2). The results showed that, like the previous research [8, 28], extraction of copper rises by raising the temperature and the concentration of ionic liquid, and none of the ionic liquids are superior to each other at temperatures lower than 40°C. However, at higher temperatures (concentration of 50%), the second ionic liquid, i.e., IL_2, showed higher copper extraction percentage than the first one, i.e., IL_1. These researchers also conducted measurements on the acidity and concentration of the $HSO4^-$ anion, the results of which indicated that acidity did not play a significant role in increasing copper extraction in the presence of ionic liquids. They concluded that the ionic liquid reduces friction between the solid and liquid phases. This reduction makes it easier for electrons to penetrate and allows for continuous acidic leaching on the solid surface. Claudia et al. [29] investigated the leaching of primary chalcopyrite using ionic liquids [Bmim][HSO_4] along with chloride and sulfuric acid through the statistical design of the experiment. This study showed that copper extraction rate at 90°C after 24 h in the presence of 20% vol of ionic liquid and 100 g/l chlorine ions is higher than 80%. Also, these researchers showed that the temperature and the concentration of chlorine ions have a positive effect on copper extraction from chalcopyrite and their interaction creates a synergistic effect. They proposed that the addition of chlorine increases the proton activity of the HSO_4^- anion and decreases the pH to -0.3. The researchers also examined the remaining solid residue from leaching using SEM-EDX. Their

investigations unveiled that in the presence of Cl^-, sulfide undergoes oxidation and transforms into elemental sulfur, and a tiny percentage of copper remains in the leaching residue; as a result, the equation proposed by previous researchers [28] is confirmed. The measured activation energy for the reaction of chalcopyrite dissolution in ionic liquids was 60.4 kJ/mol, which showed that this reaction is controlled chemically. In 2020, Rodríguez et al. conducted studies on the leaching of chalcopyrite with sodium bromide and the ionic liquid [Bmim]HSO_4 [30]. They showed that 85% copper extraction can be reached at 90 °C, with 20% (*v*/*v*) of ionic liquid and 100 g/l bromide. Under this condition, the activation energy was 75.73 kJ/mol, which showed that the chemical reaction controls chalcopyrite dissolution. The dissolution of chalcopyrite using ionic liquid with various cations and anions, alongside the utilization of potassium dichromate as an oxidizer, was examined and studied by Ho et al [31]. For this purpose, they employed ionic liquids containing $Bmim^+$ cation paired with different anions ($CF_3SO_3^-$, BF_4^-, NTf_2^-, PF_6^-, and HSO_4^-) as well as ionic liquids containing HSO_4^- anion paired with various cations ($[Omim]^+$, $[Hmim]^+$, $[Bmim]^+$, and $[Emim]^+$). The results showed that the highest copper extraction rate is obtained among different anions and cations in the presence of HSO_4^- anion and $[Emim]^+$ cation. Therefore, they suggested the use of 1-ethyl-3-methyl-imidazolium hydrogen sulfate ([Emim]HSO_4) ionic liquid for chalcopyrite dissolution. They also showed that the chalcopyrite dissolution rate rises with raising the [Emim]HSO_4 concentration, potassium dichromate, and temperature. The investigation of the dissolution kinetic mechanism by these researchers also showed that the dissolution of chalcopyrite follows the diffusion mechanism from the produced layer with an activation energy of 36.26 kJ/mol.

According to the research, it can be seen that ionic liquids have a significant effect on the dissolution of chalcopyrite. In addition, achieving high copper extraction rates from chalcopyrite using ionic liquids requires the use of oxidizers such as H_2O_2, $K_2Cr_2O_7$, $(NH_4)_2S_2O_8$, HClO, $NaClO_3$, KNO_3 and Fe_3^+ [31-33]. Among these oxidizers, H_2O_2 is an environmentally friendly oxidizer because it turns into water and oxygen after the reaction and does not produce additional pollutants [34]. Also, little research has been done on the interaction effect of various parameters including temperature, speed of stirring, ionic liquid and oxidizer concentration, size of particle, and ratio of solid-to-liquid on the chalcopyrite dissolution rate. Consequently, in this study, [Bmim][HSO_4] ionic liquid was selected owing to its advantageous, including water solubility, cost-effectiveness, and widespread availability, along with H_2O_2 as an environmentally friendly oxidizing agent to investigate the dissolution of chalcopyrite by applying the experiment design method. The impact of various operating factors on chalcopyrite leaching was assessed, including the concentration of ionic liquid and oxidizer, ratio of solid-to-liquid, temperature, speed of stirring, and possible interactions affecting. Also, the kinetics of chalcopyrite leaching and the effect of operational parameters on the kinetics were investigated by the shrinking core model.

EXPERIMENTAL SECTION

Characteristics of the chalcopyrite concentrate

The research utilized chalcopyrite concentrate sourced from the Taknar Copper Mines Complex flotation unit in Razavi Khorasan, Iran. The samples underwent analysis using X-ray diffraction (XRD), X-ray fluorescence (XRF), and microscopic mineralogy methods to identify the main minerals and elements present. Fig. 1(a) shows the XRD pattern of chalcopyrite concentrate. It can be seen that the main constituent mineral of this sample is chalcopyrite, along with a small amount of pyrite. Also, the microscopic mineralogy studies showed tiny amounts of copper oxide minerals, chalcocite, and bornite. The amount of copper in these minerals was estimated to be

less than 5%. Therefore, the dominant compounds of copper in the sample are acid-resistant sulfide, which cannot be easily dissolved by acid.

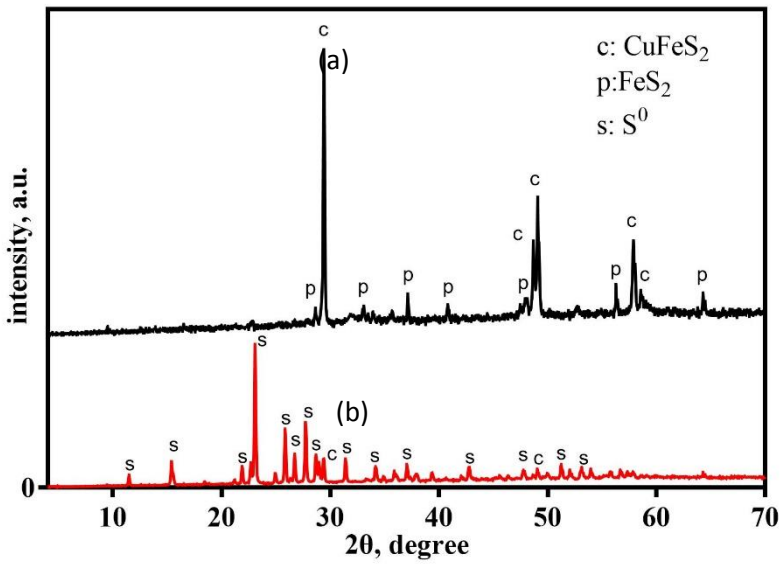

Fig. 1: X-ray diffraction pattern of : (a) concentrate of chalcopyrite after leaching, (b) leached concentrate under the optimized condition.

The XRF and chemical analysis results for the target sample, categorized into four fractions (-88, +74), (-74, +53), (-53, +37), and below 37 microns through wet sieving, are presented in Table 1. The high iron and sulfur content detected in this sample confirms the presence of copper sulfide minerals (chalcopyrite).

Table 1: Composition of the CuFeS2 concentrate and each size fraction.

Size fraction (µm)	*Cu (%)*	*Fe (%)*	*S (%)*
-37	*30.7*	*27.6*	*32.6*
(-53 , +37)	*29.1*	*30.2*	*32.5*
(-74 , +53)	*27.8*	*30.7*	*31.5*
(-88 , +74)	*29.1*	*28.5*	*30.6*

Chemicals reagents

ionic liquid 1-butyl-3-methyl-imidazolium hydrogen sulfate ([Bmim][HSO_4], purity of ≥ 94.5%) was supplied from Sigma Aldrich Co. Hydrogen peroxide (H_2O_2, 35 wt%) was purchased from Merck Co. Distilled water was used in all the experiments.

Design of experiments

Since several factors can affect the leaching process, optimizing the process to achieve the product with the desired specifications requires accurate tests and precise analysis of the results. Today, statistical methods are used for designing and analyzing the results of experiments. These methods take into account the independent factors as well as potentially effective interactions. For this reason, the design expert software was used in this research to design and analyze the results of the experiments. For investigating the effect of each parameter (including

temperature, speed of stirring, concentration of [Bmim][HSO_4] ionic liquid and H_2O_2, speed of stirring, and ratio of solid-to-liquid) and their interactions, and also optimizing the operating parameters, 32 experiments (N = $2^{(5-1)}$ + (2 ×5) + 6 = 30) including 16 experiments based on fractional factorial design ($2^{(5-1)}$), 10 experiments based on axial points (2×5), and 6 experiments based on central points were designed and implemented using the central composite design (CCD) layout of the response surface method (RSM) matrix. In this design, copper extraction was considered as the response. The functional relationship in RSM is often represented by two important models: the first-degree polynomial model (equation 4) and the second-degree polynomial model (equation 5).

$$Y = a_0 + \sum_{i=1}^{n} a_i X_i + \varepsilon \quad (4)$$

$$Y = a_0 + \sum_{i=1}^{kn} a_i X_i + \sum_{i=1}^{kn} a_{ii} X_i^2 + \sum_{1 \le i \le j}^{n} a_{ij} X_i X_j + \varepsilon \quad (5)$$

In the given equation, Y represents the predicted response, which in this case is the copper extraction rate. a_0, a_i, a_{ii}, and a_{ij} represents the coefficient of constant, linear, quadratic, and interaction, respectively. X_i and X_j represent the independent variables coded values, while X_iX_j represents the interaction terms and X_i^2 represents the quadratic terms. The variable k also denotes the number of independent variables being studied (in this study, n = 5). The parameters and their corresponding levels are outlined in Table 2. It should be noted that the selection of parameter levels was determined through a series of preliminary tests and a comprehensive review of prior research conducted in this field.

Table 2 Central-Composite Design factor levels of independent variables.

Factor	*Units*	*Notation*	*Coded variable levels*				
			-2	*-1*	*0*	*1*	*-2*
BmimHSO₄ concentration	***%(w/v)***	***A***	***10***	***20***	***30***	***40***	***50***
H_2O_2 concentration	***%(v/v)***	***B***	***15***	***20***	***25***	***30***	***35***
temperature	***°C***	***C***	***25***	***30***	***35***	***40.***	***45***
solid-to-liquid ratio	***g/l***	***D***	***5***	***10***	***15***	***20***	***25***
stirring speed	***rpm***	***E***	***100***	***200***	***300***	***400***	***500***

Leaching experiments

After designing the experiments, all the leaching experiments were performed in a 50 ml Erlenmeyer flask. To stir and heat the leaching solution, a Deragoon MS7 H550Pro magnetic hot plate equipped with a PT1000 temperature sensor was used for more accurate control and stabilization of the solution temperature.

To perform these experiments, specific concentrations of the [Bmim][HSO_4] ionic liquid solution and H_2O_2 oxidizer were heated on a magnetic hot plate. After the temperature of the solution reached the desired level, a specific amount of the chalcopyrite concentrate was added to the solution. Then, the magnetic stirrer was turned on at a specified speed, and the leaching process continued for the desired period. After the completion of each test, the studied sample was filtered, and its solution phase was analyzed to determine the amount of copper using an atomic absorption spectrometer (Varian-AA240). The percentage of copper extraction was calculated according to Equation (6) [35].

$$R = \frac{V.c}{F.f} \times 100 \quad (6)$$

In the given equation, R represents the copper extraction percentage (%), V denotes the volume of the leaching solution in the Erlenmeyer flask (ml), c indicates the copper concentration in the solution (g/ml), F represents the weight of the chalcopyrite concentrate (g), and f signifies the percentage of copper in the chalcopyrite concentrate.

RESULTS AND DISCUSSION

Data analysis

The values of the test variables, namely [Bmim][HSO_4] concentration (parameter A, w/v%), H_2O_2 concentration (parameter B, v/v%), temperature (parameter C, ºC), solid-to-liquid ratio (parameter D, g/l), stirring speed (parameter E, rpm) and the design of experiments and the results are shown in Table 3.

Table 3: Experimental plan and matrix in coded units and experimental responses.

Standard Run No.	*Independent variable in coded form*					*Cu extraction (%)*
	A	*B*	*C*	*D*	*E*	
1	*-1*	*-1*	*-1*	*-1*	*1*	*45.4856*
2	*1*	*-1*	*-1*	*-1*	*-1*	*42.8656*
3	*-1*	*1*	*-1*	*-1*	*-1*	*35.3523*
4	*1*	*1*	*-1*	*-1*	*1*	*66.8966*
5	*-1*	*-1*	*1*	*-1*	*-1*	*50.4622*
6	*1*	*-1*	*1*	*-1*	*1*	*61.4877*
7	*-1*	*1*	*1*	*-1*	*1*	*68.38*
8	*1*	*1*	*1*	*-1*	*-1*	*88.9129*
9	*-1*	*-1*	*-1*	*1*	*-1*	*42.6845*
10	*1*	*-1*	*-1*	*1*	*1*	*36.5804*
11	*-1*	*1*	*-1*	*1*	*1*	*44.0078*
12	*1*	*1*	*-1*	*1*	*-1*	*46.3747*
13	*-1*	*-1*	*1*	*1*	*1*	*42.7325*
14	*1*	*-1*	*1*	*1*	*-1*	*54.9284*
15	*-1*	*1*	*1*	*1*	*-1*	*62.2764*
16	*1*	*1*	*1*	*1*	*1*	*88.5477*
17	*-2*	*0*	*0*	*0*	*0*	*50.1008*
18	*2*	*0*	*0*	*0*	*0*	*70.5475*
19	*0*	*-2*	*0*	*0*	*0*	*34.3926*
20	*0*	*2*	*0*	*0*	*0*	*70.657*
21	*0*	*0*	*-2*	*0*	*0*	*31.1931*
22	*0*	*0*	*2*	*0*	*0*	*62.1204*
23	*0*	*0*	*0*	*-2*	*0*	*72.601*
24	*0*	*0*	*0*	*2*	*0*	*63.5768*
25	*0*	*0*	*0*	*0*	*-2*	*46.8246*
26	*0*	*0*	*0*	*0*	*2*	*55.1079*
27	*0*	*0*	*0*	*0*	*0*	*72.6471*
28	*0*	*0*	*0*	*0*	*0*	*68.4808*
29	*0*	*0*	*0*	*0*	*0*	*70.0865*
30	*0*	*0*	*0*	*0*	*0*	*66.7433*
31	*0*	*0*	*0*	*0*	*0*	*71.6693*
32	*0*	*0*	*0*	*0*	*0*	*68.4942*

The model's adequacy was assessed by using the sum of squares from the sequential model. A summary of the model's statistics can be found in Table 4.

Table 4: Statistical analysis of models for predicting the Cu extraction.

Source	*Sum of Squares*	*df*	*Mean Squares*	*F-value*	*P-value*	*Remark*
						Sequential Model Sum of Squares
Mean vs Total	***1.073E+05***	***1***	***1.073E+05***			
Linear vs Mean	***4618.02***	***5***	***923.60***	***9.22***	***< 0.0001***	
2FI vs Linear	***935.77***	***10***	***93.58***	***0.8973***	***0.5562***	
Quadratic vs 2FI	***1575.52***	***5***	***315.10***	***37.21***	***< 0.0001***	***Suggested***
Cubic vs Quadratic	***38.01***	***5***	***7.60***	***0.8269***	***0.5733***	***Aliased***
Residual	***55.15***	***6***	***9.19***			
Total	***1.145E+05***	***32***	***3579.63***			
						Model Summary Statistics
Source	***Std. Dev.***	***R^2***	***Adjusted R^2***	***Predicted R^2***	***PRESS***	
Linear	***10.01***	***0.6394***	***0.5700***	***0.4709***	***3821.69***	
2FI	***10.21***	***0.7690***	***0.5524***	***-0.4785***	***10678.09***	
Quadratic	***2.91***	***0.9871***	***0.9636***	***0.7567***	***1756.95***	***Suggested***
Cubic	***3.03***	***0.9924***	***0.9605***	***-3.6272***	***33419.66***	***Aliased***

df =Degree of freedom

As can be seen, the regression coefficient of the quadratic model is 0.9871. The adjusted R^2 and the predicted R^2 for the quadratic model are 0.9636 and 0.7567, respectively. These results indicate that the model adequately and fits the experimental data equally well. In conclusion, the experimental data was analyzed using a quadratic polynomial model as outlined in Equation (5). After removing insignificant terms with a p-value greater than 0.05, the model was developed and expressed in Equation (6).

$$R= +69.29 +5.67A +8.17B +9.14C -2.49D +1.95E +4.14AB +2.80AC +4.59BC +2.47BE - 1.86A^2 -3.81B^2 -5.28C^2 -4.20E^2 \quad (6)$$

All the variables mentioned are represented by coded values ranging from -2 to 2. The analysis of variance (ANOVA) results for fitting quadratic models to the experimental data are presented in Table 5.

The ANOVA results indicate the significant contribution of the quadratic model. The significance of each coefficient was evaluated by both the F-test and P-test, as outlined in Table 5. In statistical analysis, a greater absolute F-value and a smaller P-value indicate the higher significance of the corresponding variable. According to the results of ANOVA (Table 5), the [Bmim][HSO_4] concentration, H_2O_2 concentration, temperature, quadratic effect of H_2O_2 concentration, temperature, and stirring speed, the interaction between [Bmim][HSO_4] concentration and H_2O_2 concentration, and the interaction between H_2O_2 concentration and temperature have the most significant effects on the $CuFeS_2$ leaching efficiency.

Table 5: ANOVA of the second order model developed.

Source	*Sum of Squares*	*df*	*Mean Square*	*F-value*	*p-value*	
Model	***7028.46***	***13***	***540.65***	***50.16***	***< 0.0001***	***significant***
A-BmimHSO$_4$ concentration	***771.87***	***1***	***771.87***	***71.61***	***< 0.0001***	
B-H$_2$O$_2$ concentration	***1601.49***	***1***	***1601.49***	***148.59***	***< 0.0001***	
C-temperature	***2004.49***	***1***	***2004.49***	***185.98***	***< 0.0001***	
D- solid to liquid ratio	***148.80***	***1***	***148.80***	***13.81***	***0.0016***	
E-stirring speed	***91.37***	***1***	***91.37***	***8.48***	***0.0093***	
AB	***274.05***	***1***	***274.05***	***25.43***	***< 0.0001***	
AC	***125.66***	***1***	***125.66***	***11.66***	***0.0031***	
BC	***337.56***	***1***	***337.56***	***31.32***	***< 0.0001***	
BE	***97.86***	***1***	***97.86***	***9.08***	***0.0075***	
A^2	***102.73***	***1***	***102.73***	***9.53***	***0.0064***	
B^2	***429.85***	***1***	***429.85***	***39.88***	***< 0.0001***	
C^2	***824.03***	***1***	***824.03***	***76.45***	***< 0.0001***	
E^2	***522.14***	***1***	***522.14***	***48.44***	***< 0.0001***	
Residual	***194.01***	***18***	***10.78***			
Lack of Fit	***169.61***	***13***	***13.05***	***2.67***	***0.1424***	***not significant***
Pure Error	***24.39***	***5***	***4.88***			
Cor Total	***7222.46***	***31***				
Statistical analysis summary						
R^2	***0.9731***		***Std. Dev.***	***3.28***		
Adjusted R^2	***0.9537***		***PRESS***	***776.74***		
Predicted R^2	***0.8925***		***C.V. %***	***5.67***		
Adeq Precision	***27.9468***		***Mean***	***57.91***		

P-values less than 0.05 indicate higher significance of the model, while P-values more than 0.5 are usually considered insignificant. Lack of Fit (LOF) is also given in Table 5 to check the fitted models' quality. At the 95% confidence level, the value of R^2 was about 0.9731, which shows that the model is suitable for predicting the chalcopyrite leaching process. In addition, the difference between the predicted R^2 and adjusted R^2 is less than 0.0612. The results demonstrate that the model is free from irrelevant terms and shows a strong correlation between test and standard estimations. These findings are further supported by the plots in Fig. 2, which illustrate the residual normal probability (Fig. 2(a)), predicted values (Fig. 2(b)), internally studentized residual values as a function of run number (Fig. 2(c)), and experimental data (measured recoveries) among the predicted values (Fig. 2(d)). It is evident from these plots that the developed model has a high capability for predicting Cu extraction

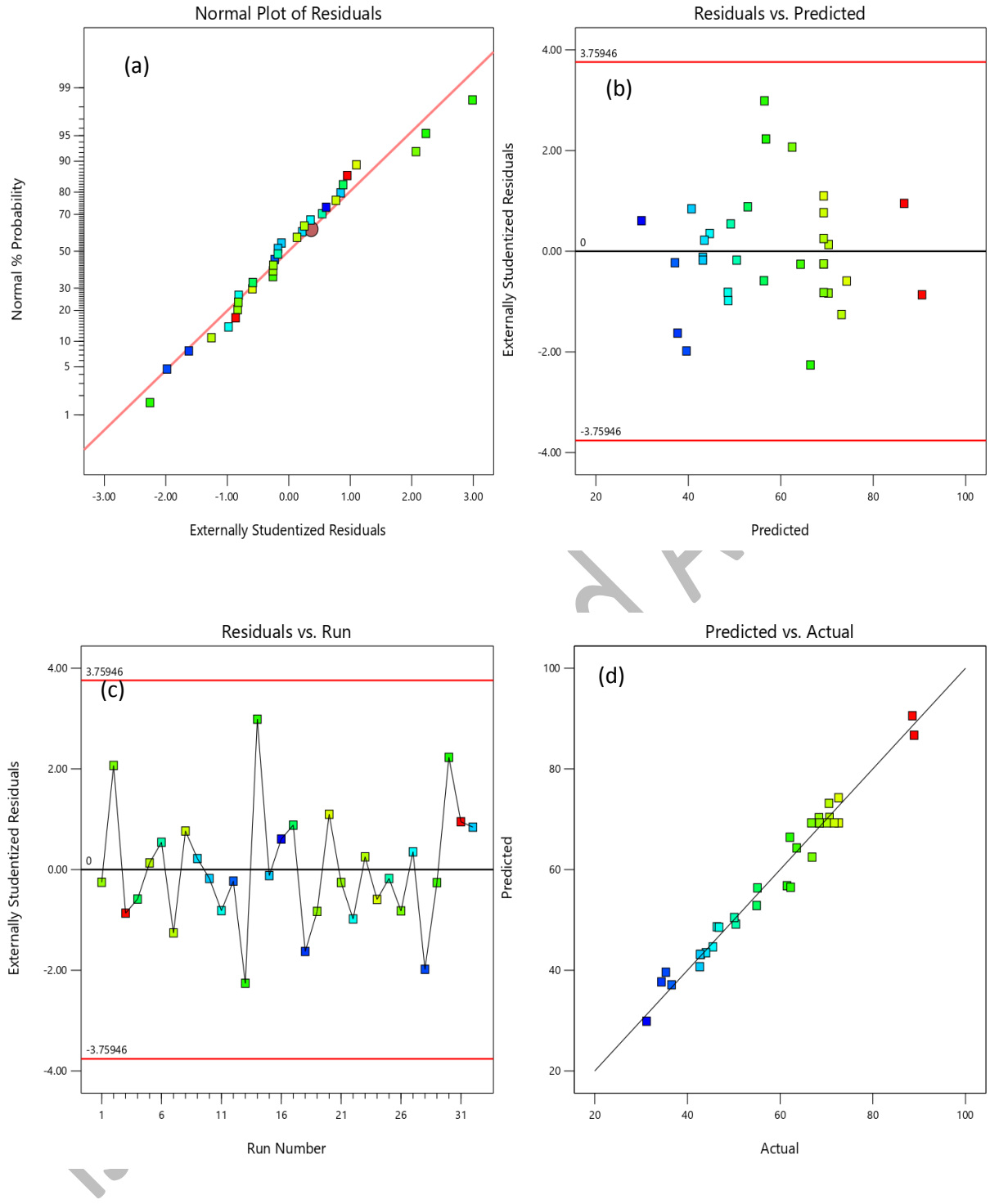

Fig. 2: Reliability of the suggested quadratic model for the prediction of Cu extraction.

Effect of parameters

The $CuFeS_2$ leaching efficiency perturbation plot (Fig. 3) shows the relative effects of different operating parameters on Cu extraction. The parameters used were 30% [Bmim][HSO_4] (parameter A), 25% H_2O_2 (parameter B), temperature of 35 °C (parameter C), ratio of solid-to-liquid 15 g/l (parameter D), and stirring speed of 300 rpm (parameter E).

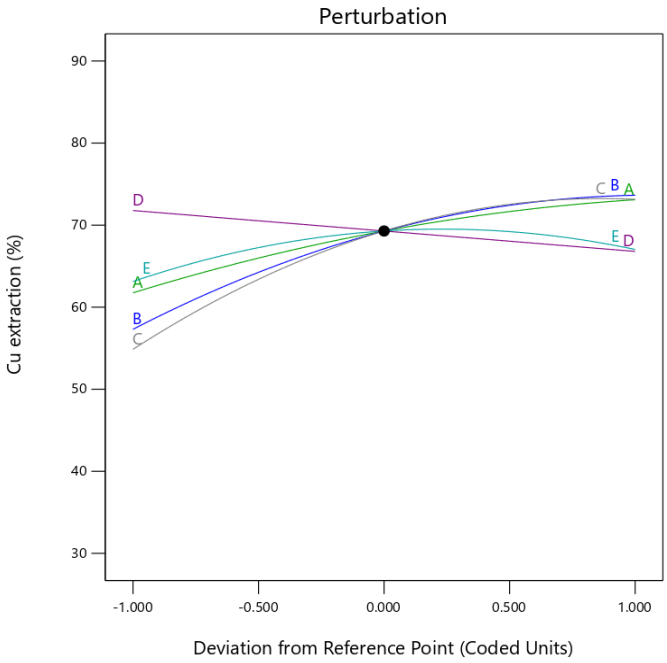

Fig. 3: Perturbation plot for Cu extraction.

By referring to Fig. 3, it is evident that the dissolution of $CuFeS_2$ increased when the concentration of [Bmim][HSO_4] was increased which may be related to the higher concentration of dissolved oxygen and the higher acidity of the solution in the presence of [Bmim][HSO_4]. Furthermore, the small increase in the dissolution of $CuFeS_2$ when the concentration of [Bmim][HSO_4] is further increased can be attributed to the rise in solution viscosity. This, in turn, limits the diffusion[8, 28].

The increase in copper extraction from $CuFeS_2$ with the higher concentration of hydrogen peroxide (H_2O_2) could be attributed to either the increased solubility of oxygen or the elevated oxidation potential of hydrogen peroxide. Furthermore, the escalation in chalcopyrite dissolution in the presence of hydrogen peroxide can be ascribed to the reaction between hydrogen peroxide and mineral substances, as depicted by reaction (7). This reaction leads to the decomposition of hydrogen peroxide into hydroxide ions (OH^-) and hydroxyl radicals (HO^+). The hydroxyl radical (HO^+) reacts with chalcopyrite by reaction (8), creating elemental sulfur. Elemental sulfur is also transformed into sulfate ions by reaction (9), and ultimately, following reaction (10), copper ions react with sulfate ions, resulting in the formation of an aqueous solution of copper sulfate [36].

$$H_2O_2 \rightarrow HO^+ + OH^- \quad (7)$$

$$2HO^+ + 2S^{2-} \rightarrow 2S^0 + H_2O + 0.5O_2 \quad (8)$$

$$2S^0 + 2H_2O + 3O_2 \rightarrow 2SO_4^{2-} + 4H^+ \quad (9)$$

$$Cu^{2+}(aq) + SO_4^{2-}(aq) \rightarrow CuSO_4(aq) \quad (10)$$

It is clear from Fig. 3 that the leaching efficiency of $CuFeS_2$ increases as the H_2O_2 concentration rises. However, after reaching its peak, the efficiency decreases at higher H_2O_2 concentrations. This may be because the

decomposition of H_2O_2 is directly related to its concentration. When the concentration of H_2O_2 is higher, its decomposition rate also increases [34, 37, 38].

According to Fig. 3, it can be seen that the leaching efficiency of $CuFeS_2$ increases with the increase in the temperature up to a certain point and then decreases because, as confirmed by other researchers, the dissolution rate of chalcopyrite slows down as a result of lower concentration of H_2O_2 in the solution at higher temperatures [39, 40]. The findings suggest that increasing the solid-to-liquid ratio does not enhance leaching efficiency. This phenomenon could be attributed to the reduced amount of leaching solution per unit mass of solids [41, 42], resulting in increased viscosity and greater resistance to mass transfer [43].

Increasing the stirring speed initially led to an increase in the dissolution of $CuFeS_2$. However, a further slight increase in stirring speed resulted in a decrease in $CuFeS_2$ dissolution. This phenomenon can be attributed to the higher stirring speed accelerating the decomposition of H_2O_2 and impeding its absorption on the chalcopyrite surface. As a result, the dissolution rate significantly decreases [39]. Sokić et al. [34] also reported that faster stirring increased the rate of H_2O_2 decomposition, causing more generated O_2 molecules to be absorbed onto the $CuFeS_2$ surface.

Interaction of parameters

Fig. 4 displays contour and three-dimensional (3D) surface plots of the quadratic model's response surface. These plots provide a visual representation of how the variables interact with each other. In these plots, two variables are changed within the experimental ranges while the remaining variables are held constant [44].

Fig. 4(a,b) and Fig. 4(c,d), respectively, show the mutual effect of [Bmim][HSO_4] concentration and H_2O_2 concentration, as well as the mutual effect of [Bmim][HSO_4] concentrations and temperature, on Cu extraction. It can be observed that increasing H_2O_2 concentration and temperature improves Cu extraction for all [Bmim][HSO_4] concentrations. In addition, at higher [Bmim][HSO_4] concentrations, the plots are steeper. Increasing Cu extraction in the presence of hydrogen peroxide can be ascribed to the reaction (7)-(10).

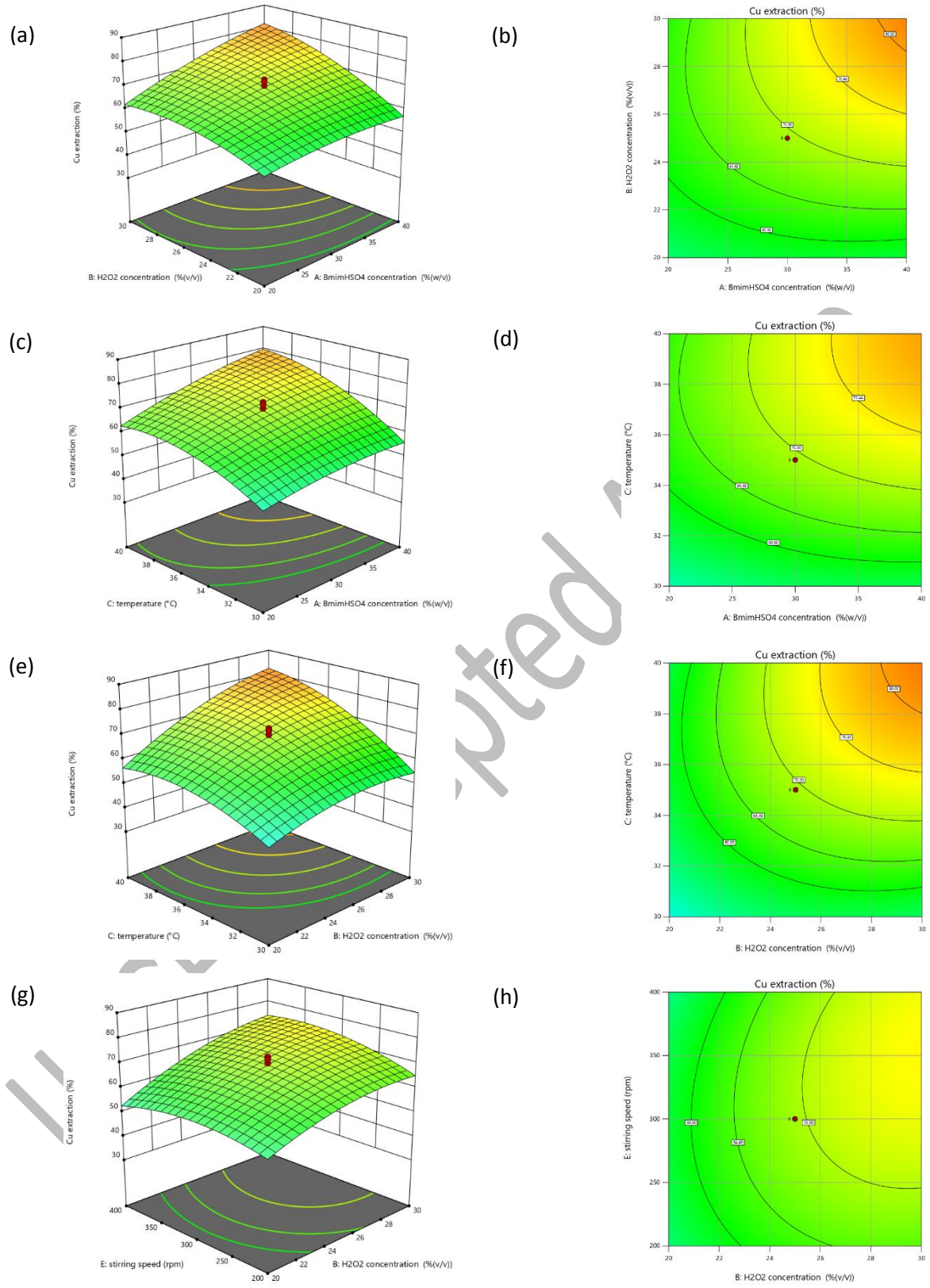

Fig. 4: 3D response surface and contour plots showing the relationship between Cu extraction leaching parameters ([Bmim][HSO$_4$] concentration, H_2O_2 concentration, temperature, and stirring speed).

Fig. 4(e,f) and Fig. 4(g,h), respectively, show the mutual effect of H_2O_2 concentration and temperature as well as the mutual effect of H_2O_2 concentration and stirring speed, on the extraction of Cu. It can be observed that

increasing temperature and stirring speed improves Cu extraction for all H_2O_2 concentrations. It can also be observed that at higher H_2O_2 concentrations, the plots are steeper. The reason for this is that The decomposition of H_2O_2 is accelerated by increasing the stirring speed and temperature [34, 37, 39].

Optimization and confirmation test

The Design Expert software was used to analyze the quadratic model of the response surface, which led to determining the optimal leaching conditions through RSM optimization. The resulting optimal conditions are as follows: [Bmim][HSO_4] concentration = 40% (w/v), H_2O_2 concentration = 30% (v/v), temperature = 40 ºC, solid-to-liquid ratio = 10 g/l, and stirring speed = 300 rpm .Under these conditions, the predicted Cu extraction efficiency was 90.57% with a desirability value of around 93%. Three leaching tests were conducted under optimal conditions to assess the practicality and accuracy of the optimized result. The average Cu extraction achieved 90.32%, which was very good and agreed with the predicted Cu extraction.

Kinetic Analysis

The reaction of chalcopyrite and ionic liquid solution come into contact during the leaching process is an example of a common type of reaction known as liquid and solid heterogeneous reactions (including non-porous and dense materials). In these processes, the reaction kinetics can usually be interpreted by the Shrinking Core Model (SCM), and the dissolution process can be described by Equation (2).

In this case, the reaction rate can be described by one of the following relationships [45, 46]:

i) If penetration and diffusion through ash/product layer controlled the reaction rate, Equation (11) can be used to express the dissolution rate.

ii) If chemical reaction controlled the reaction rate, Equation (12) can be used to express the dissolution rate.

$$1-3(1-x)^{\frac{2}{3}}+2(1-x)=k_d t \quad (11)$$

$$1-(1-x)^{\frac{1}{3}}=k_r t \quad (12)$$

Where x denotes the fraction of copper leached, t depicts the leaching time (min), and kr and kd are the apparent rate constants of surface chemical model and product layer diffusion (min^{-1}), respectively.

Due to the significant difference in the resistance of these steps, the step that creates the highest resistance to the reaction is called the controller or limiter of the reaction rate [33, 46]. In order to check the compatibility of the chalcopyrite dissolution process with the mentioned mechanisms, equations related to the limiting steps were plotted versus time in the studied temperature range. Fig. 5(a and b) show the graphs obtained from Equations (11) and (12), respectively. According to the correlation coefficient (R^2) of the experimental data in these graphs, the correlation coefficient for reaction control via chemical reaction is closer to one than the correlation coefficient for reaction control through diffusion. Therefore, it can be concluded that Equation (12) better describes the data obtained from the experiments, and the mechanism of the leaching process is more compatible with the chemical reaction mechanism.

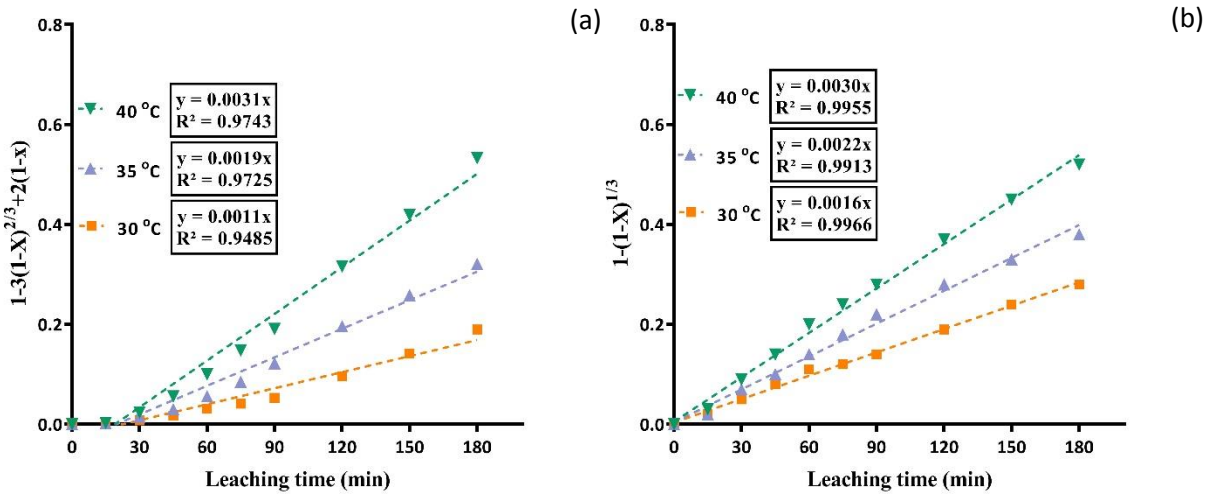

Fig. 5: Plot of (a) $1-(1-x)^{\frac{1}{3}}$***, (b)*** $1-3(1\text{-}x)^{\frac{2}{3}}+2(1\text{-}x)$ ***vs. time for dissolution of*** $CuFeS_2$ ***at different temperatures.***

The slope of $1-(1-x)^{\frac{1}{3}} = kt$ plot versus time at different temperatures (Fig. 5 b) determines the value of the kinetic constant (k_p). The activation energy can be determined by using the slopes and the Arrhenius law, which is described by Equation 13[33].

$$\ln K_p = \ln A - \left(\frac{-E_a}{RT}\right) \qquad (13)$$

Where k_p represents the rate constant, A stands for the frequency factor, E_a denotes the activation energy (KJ/mol), R represents the universal gas constant, and T signifies the absolute temperature (K). Equation (13) states that the slope of the lnkp curve versus 1/T is equal to -Ea/R. By multiplying this value by -R, we can determine the amount of activation energy. As seen in Fig. 6, the slope of this curve is -5.9674. Therefore, the activation energy is 49.61 kJ/mol.

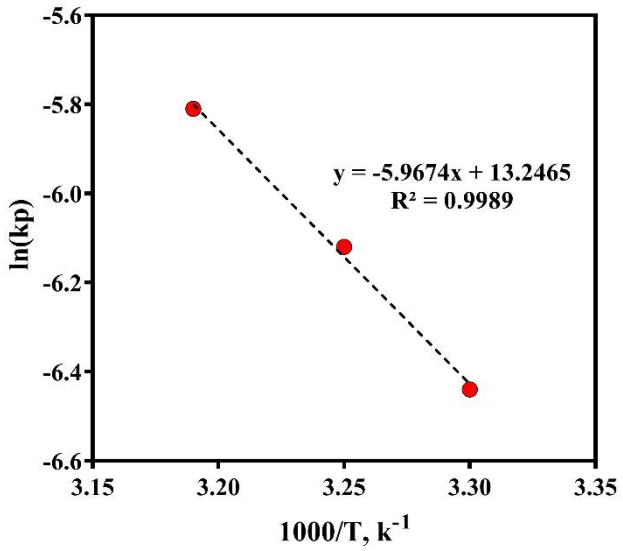

Fig. 6: Arrhenius plot obtained for Cu extraction.

Considering that the low activation energy (less than 20 kJ/mol) is attributed to reaction control by diffusion and the high activation energy (more than 40 kJ/mol) is related to reaction control by chemical reaction [32], It can be concluded that the leaching process of chalcopyrite using the ionic liquid [Bmim][HSO4] follows the chemical reaction mechanism.

Surface Studies

After optimization experiments, the leaching residue was analyzed using SEM/EDS and XRD analyses. The XRD analysis (Fig. 1 a) confirms that elemental sulfur is formed during the leaching process. The results of SEM and EDS analyses of the chalcopyrite concentrate and the leaching residue are shown in Fig. 7(a,b) and Fig. 7(c,d), respectively. As can be seen in Fig. 7(a), the surface of chalcopyrite particles is free of any layer, and the EDS analysis (Fig. 7(b)) confirms the presence of chalcopyrite. However, Fig. 7(c) shows the formation of a layer with a different structure. Also, EDS analysis (Fig. 7(d)) shows that sulfur has the highest concentration in the leaching residual solid. These results indicate that most of the chalcopyrite is dissolved, and the high activation energy can arise from forming the elemental sulfur layer.

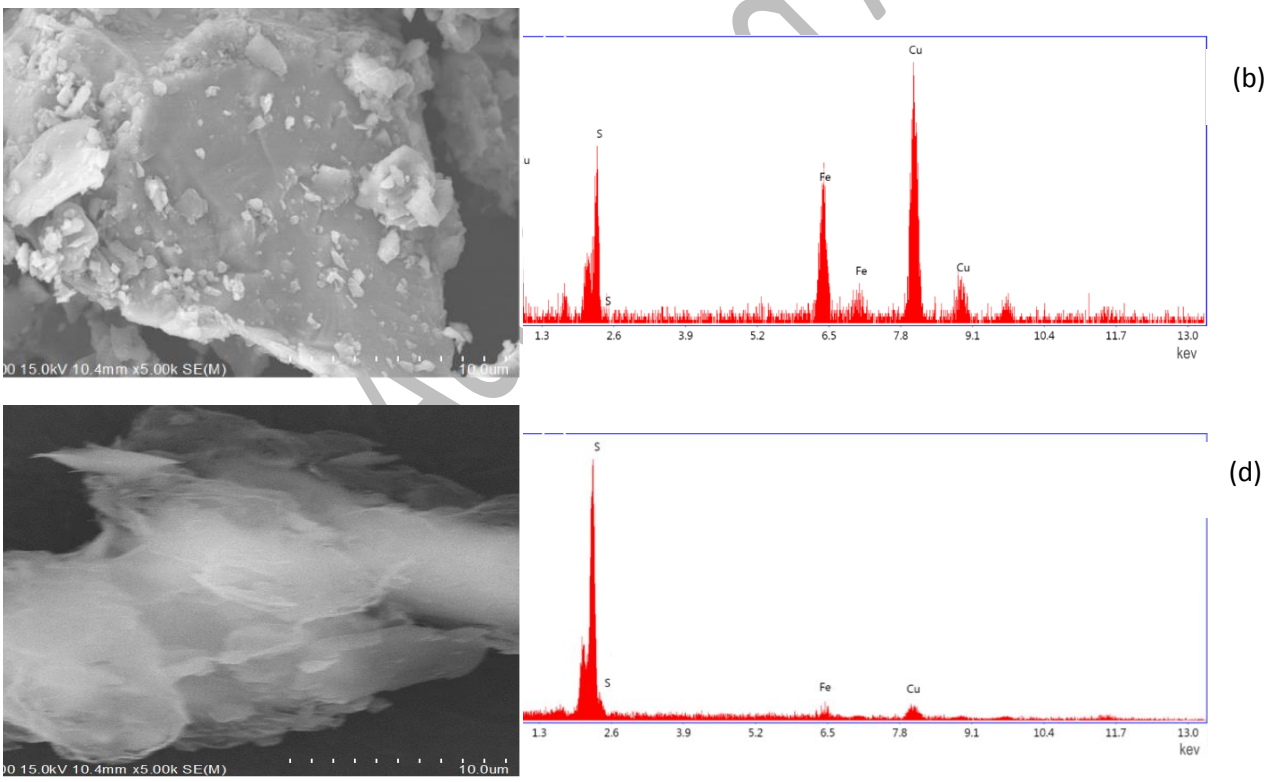

Fig. 7: (a) SEM micrograph of feed $CuFeS_2$ particle, (b) EDX micrograph of feed $CuFeS_2$ particle, (c) SEM micrograph of leached particle, (d) EDX micrograph of leached particle.

The dominant mechanism of chalcopyrite dissolution by H_2O_2 in acidic solution can be expressed according to reaction (14). However, at the same time, according to reaction (15), a small amount of sulfur in sulfide is oxidized. The sum of reactions (14) and (15) can be written as reaction (16) [34]. Considering the above reactions, the structure of chalcopyrite particles, and the analysis of the leaching residue, it can be concluded that the dissolution

reaction of chalcopyrite in the presence of [Bmim][HSO_4] ionic liquid and H_2O_2 oxidizer can be written as reaction (16).

$$2CuFeS_2 + 17H_2O_2 + 2H^+ \rightarrow 2Cu^{2+} + 2Fe^{3+} + 4SO_4^{2-} + 18H_2O \quad (14)$$

$$4SO_4^{2-} + 2H^+ + 2H_2O \rightarrow S^0 + 3H_2O_2 \quad (15)$$

$$2CuFeS_2 + 5H_2O_2 + 10^{H+} \rightarrow 2Cu^{2+} + 2Fe^{3+} + 4S^0 + 10H_2O \quad (16)$$

CONCLUSIONS

In this paper, leaching of chalcopyrite was conducted in the presence of [Bmim][HSO_4] ionic liquid by applying the experiment design method using the central composite design (CCD) layout of the response surface method (RSM) matrix. The influence of temperature, speed of stirring, concentration of [Bmim][HSO_4] and H_2O_2, ratio of solid-to-liquid, and their interactions on chalcopyrite leaching were investigated. The equation of the proposed model, developed using the response surface method (RSM), has a correlation coefficient (R^2) of 0.9731, which indicates a significant level of consistency with the experimental data. Among the investigated parameters, temperature, oxidizer concentration, and ionic liquid concentration had the most significant effect on the Cu extraction. The interaction of oxidizer concentration with temperature and concentration of ionic liquid had the most significant effect on the dissolution rate of chalcopyrite. In other words, at high oxidizer concentrations, the chalcopyrite dissolution rate significantly increased with increasing the temperature and ionic liquid concentration. The highest Cu extraction rate of 90.32% was obtained at 40°C using 40% [Bmim][HSO_4], 30% H_2O_2, solid-to-liquid ratio of 10 g/l, and stirring speed of 300 rpm. Examination of the chalcopyrite leaching residue showed that most of the chalcopyrite has been dissolved, and sulfur is the major constituent of the leaching residue. Kinetic studies using the shrinking core method showed that the mechanism of chalcopyrite leaching in the presence of [Bmim][HSO_4] ionic liquid and H_2O_2 oxidizer follows the chemical reaction mechanism. This mechanism can be expressed by the 1-(1-x)1/3=kt equation which leads to the activation energy of 49.61 kJ/mol.

Acknowledgements

The authors extend their sincere gratitude to the laboratories of mineral processing, X-ray, and geochemistry at the University of Tehran for their invaluable support.

REFERENCES

[1] Nazari G., Asselin E., Morphology of chalcopyrite leaching in acidic ferric sulfate media, *Hydrometallurgy*, **96**(3): 183-188 (2009).

[2] Zandevakili S., Akhondi M.R., Hosseini R., Mohammad S., Leaching optimization of Sarcheshmeh copper concentrate by application of Taguchi experimental design method, *Iran. J. Chem. Chem. Eng. Research Article Vol*, **39**(6): 229-236 (2020).

[3] Watling H., Chalcopyrite hydrometallurgy at atmospheric pressure: 2. Review of acidic chloride process options, *Hydrometallurgy*, **146**(3): 96-110 (2014).

[4] Radmehr V., Koleini S.M.J., Khalesi M.R., Mohammadi M.R.T., Ammonia Leaching: A new approach of copper industry in hydrometallurgical processes, *Journal of The Institution of Engineers (India): Series D*, **94**(2): 95-104 (2013).

[5] Yavari M., Ebrahimi S., Aghazadeh V., Ghashghaee M., Intensified bioleaching of copper from chalcopyrite: decoupling and optimization of the chemical stage, *Iranian Journal of Chemistry and Chemical Engineering*, **39**(5): 343-352 (2020).

[6] Padilla R., Vega D., Ruiz M., Pressure leaching of sulfidized chalcopyrite in sulfuric acid–oxygen media, *Hydrometallurgy*, **86**(1-2): 80-88 (2007).

[7] Anderson C., Dahlgren E., Huang H., Miranda P., Stacey D., Jeffrey M., Chandra I., Fundamentals and applications of alkaline sulfide leaching and recovery of gold, *CIM Gold Symposium, Calgary, Alberta*, **43**(2): 145-164 (2005).

[8] Whitehead J., Zhang J., Pereira N., McCluskey A., Lawrance G., Application of 1-alkyl-3-methyl-imidazolium ionic liquids in the oxidative leaching of sulphidic copper, gold and silver ores, *Hydrometallurgy*, **88**(1-4): 109-120 (2007).

[9] Barton I.F., Hiskey J.B., Chalcopyrite leaching in novel lixiviants, *Hydrometallurgy*, **207**(2): 105-775 (2022).

[10] Carlesi C., Cortes E., Dibernardi G., Morales J., Muñoz E., Ionic liquids as additives for acid leaching of copper from sulfidic ores, *Hydrometallurgy*, **161**(1): 29-33 (2016).

[11] Greaves T.L., Drummond C.J., Protic ionic liquids: properties and applications, *Chemical reviews*, **108**(1): 206-237 (2008).

[12] Blasucci V.M., Hart R., Pollet P., Liotta C.L., Eckert C.A., Reversible ionic liquids designed for facile separations, *Fluid Phase Equilibria*, **294**(1-2): 1-6 (2010).

[13] Park J., Jung Y., Kusumah P., Lee J., Kwon K., Lee C.K., Application of ionic liquids in hydrometallurgy, *International journal of molecular sciences*, **15**(9): 15320-15343 (2014).

[14] Renner R., Ionic liquids: an industrial cleanup solution, *Environmental science & technology*, **35**(19): 410A-413A (2001).

[15] Turner E.A., Pye C.C., Singer R.D., Use of ab initio calculations toward the rational design of room temperature ionic liquids, *The Journal of Physical Chemistry A*, **107**(13): 2277-2288 (2003).

[16] Yang Q., Dionysiou D.D., Photolytic degradation of chlorinated phenols in room temperature ionic liquids, *Journal of Photochemistry and Photobiology A: Chemistry*, **165**(1): 229-240 (2004).

[17] Niedermeyer H., Hallett J.P., Villar-Garcia I.J., Hunt P.A., Welton T., Mixtures of ionic liquids, *Chemical Society Reviews*, **41**(23): 7780-7802 (2012).

[18] Mallakpour S., Dinari M., Ionic liquids as green solvents: progress and prospects, *Green Solvents II*, **37**(3): 1-32 (2012).

[19] Whitehead J.A., Lawrance G.A., McCluskey A., 'Green'leaching: recyclable and selective leaching of gold-bearing ore in an ionic liquid, *Green Chemistry*, **6**(7): 313-315 (2004).

[20] Whitehead J., Zhang J., Pereira N., McCluskey A., Lawrance G., Application of 1-alkyl-3-methyl-imidazolium ionic liquids in the oxidative leaching of sulphidic copper, gold and silver ores, *Hydrometallurgy*, **88**(1): 109-120 (2007).

[21] Whitehead J., Zhang J., McCluskey A., Lawrance G., Comparative leaching of a sulfidic gold ore in ionic liquid and aqueous acid with thiourea and halides using Fe (III) or HSO_5^- oxidant, *Hydrometallurgy*, **98**(3): 276-280 (2009).

[22] Davris P., Balomenos E., Panias D., Paspaliaris I., Leaching of rare earths from bauxite residues using imidazolium based ionic liquids, *ERES2014: 1st European Rare Earth Resources Conference, Milos, Greece*, **49**(33): 241-252 (2014).

[23] Davris P., Balomenos E., Panias D., Paspaliaris I., Selective leaching of rare earth elements from bauxite residue (red mud), using a functionalized hydrophobic ionic liquid, *Hydrometallurgy*, **164**(1): 125-135 (2016).

[24] Tian G.-C., Jian L., Hua Y.-X., Application of ionic liquids in hydrometallurgy of nonferrous metals, *Transactions of Nonferrous Metals Society of China*, **20**(3): 513-520 (2010).

[25] Abbott A.P., Frisch G., Hartley J., Ryder K.S., Processing of metals and metal oxides using ionic liquids, *Green Chemistry*, **13**(3): 471-481 (2011).

[26] ABBOTT A.P., FRISCH G., Ionometallurgy: Processing of Metals using Ionic Liquids, *Element Recovery and Sustainability*, **87**(22): 59 (2013).

[27] McCluskey A., Lawrance G.A., Leitch S.K., Owen M.P., Hamilton I.C., Ionic liquids and metal ions: from green chemistry to ore refining, *ACS Symposium Series*, **818**(1): 192-212 (2002).

[28] Dong T., Hua Y., Zhang Q., Zhou D., Leaching of chalcopyrite with Brønsted acidic ionic liquid, *Hydrometallurgy*, **99**(1-2): 33-38 (2009).

[29] Aguirre C.L., Toro N., Carvajal N., Watling H., Aguirre C., Leaching of chalcopyrite (CuFeS2) with an imidazolium-based ionic liquid in the presence of chloride, *Minerals Engineering*, **99**(3): 60-66 (2016).

[30] Rodríguez M., Ayala L., Robles P., Sepúlveda R., Torres D., Carrillo-Pedroza F.R., Jeldres R.I.,Toro N., Leaching chalcopyrite with an imidazolium-based ionic liquid and bromide, Metals, **2**(2): 183-197 (2020).

[31] Hu J., Zi F., Tian G., Extraction of copper from chalcopyrite with potassium dichromate in 1-ethyl-3-methylimidazolium hydrogen sulfate ionic liquid aqueous solution, *Minerals Engineering*, **172**(1)**:** 107-179 (2021).

[32] Habashi F., "Principles of extractive metallurgy", CRC Press, (1969).

[33] Levenspiel O., "Chemical reaction engineering", John Wiley & Sons, (1999).

[34] Sokić M., Marković B., Stanković S., Kamberović Ž., Štrbac N., Manojlović V., Petronijević N., Kinetics of chalcopyrite leaching by hydrogen peroxide in sulfuric acid, *Metals*, **9**(11): 11-73 (2019).

[35] Georgiou D., Papangelakis V.J.H., Sulphuric acid pressure leaching of a limonitic laterite: chemistry and kinetics, **49**(1-2): 23-46 (1998).

[36] Olubambi P., Potgieter J., Investigations on the mechanisms of sulfuric acid leaching of chalcopyrite in the presence of hydrogen peroxide, *Mineral Processing & Extractive Metallurgy Review*, **30**(4): 327-345 (2009).

[37] PetroviĆ S.J., BogdanoviĆ G.D., AntonijeviĆ M.M., Leaching of chalcopyrite with hydrogen peroxide in hydrochloric acid solution, *Transactions of Nonferrous Metals Society of China*, **28**(7): 1444-1455 (2018).

[38] Wu J., Ahn J., Lee J., Kinetic and mechanism studies using shrinking core model for copper leaching from chalcopyrite in methanesulfonic acid with hydrogen peroxide, *Mineral Processing and Extractive Metallurgy Review*, **42**(1): 38-45 (2021).

[39] Antonijević M., Dimitrijević M., Janković Z., Leaching of pyrite with hydrogen peroxide in sulphuric acid, *Hydrometallurgy*, **46**(1-2): 71-83 (1997).

[40] Mahajan V., Misra M., Zhong K., Fuerstenau M., Enhanced leaching of copper from chalcopyrite in hydrogen peroxide–glycol system, *Minerals Engineering*, **20**(7): 670-674 (2007).

[41] Bayrak B., Laçin O., Saraç H., Kinetic study on the leaching of calcined magnesite in gluconic acid solutions, *Journal of Industrial and Engineering Chemistry*, **16**(3): 479-484 (2010).

[42] Copur M., Kizilca M., Kocakerim M.M., Determination of the optimum conditions for copper leaching from chalcopyrite concentrate ore using taguchi method, *Chemical Engineering Communications*, **202**(7): 927-935 (2015).

[43] Kim C.J., Yoon H.S., Chung K.W., Lee J.Y., Kim S.D., Shin S.M., Lee S.J., Joe A.R., Lee S.I.,Yoo S.J., Leaching kinetics of lanthanum in sulfuric acid from rare earth element (REE) slag, *Hydrometallurgy*, **146**(2): 133-137 (2014).

[44] Sabouti A., Rezai B., Hoseinian F.S., Moradkhani D., Optimization and kinetics studies of lead concentrate leaching using fluoroboric acid, *Physicochemical Problems of Mineral Processing*, **55** (4): 1014-1027 (2019).

[45] Gharabaghi M., Irannajad M., Noaparast M., A review of the beneficiation of calcareous phosphate ores using organic acid leaching, *Hydrometallurgy*, **103**(1-4): 96-107 (2010).

[46] Faraji F., Alizadeh A., Rashchi F., Mostoufi N., Kinetics of leaching: a review, *Reviews in Chemical Engineering*, **1**(ahead-of-print): **38**(2): 35-53 (2020).